Integrated Sensor Arrays based on PiezoPaint™ for SHM Applications

Karl Elkjaer[1], Konstantin Astafiev[2], Erling Ringgaard[3], and Tomasz Zawada[4]

[1,2,3,4]*Meggitt A/S, Kvistgaard, 3490, Denmark*

karl.elkjaer@meggitt.com
konstantin.astafiev@meggitt.com
erling.ringgaard@meggitt.com
tomasz.zawada@meggitt.com

ABSTRACT

Recent progress in development of new functional materials that are flexible and can be processed at very low temperatures (below 100 °C) opens a new opportunity for applications, such as non-destructive evaluation (NDE), or structural health monitoring (SHM) by applying active materials directly on the structures made out of a variety of materials, e.g. metals (aluminium), plastics, and polymers, including CFRP (Carbon Fibre Reinforced Polymer). This paper presents sensor arrays based on a flexible piezoelectric material – PiezoPaint™. The newly developed material exhibits relatively high sensitivity (d_{33} coefficient up to 45 pC/N), extremely low processing temperatures (< 120 °C), and high compliance in the cured state, enabling direct deposition of acoustic/vibration sensor arrays on structures to be monitored by means of screen- or pad-printing. The printed sensors have been applied for impact detection where four-element arrays and a fully integrated wiring system has been deposited directly on aluminium as well as CFRP plates. The presented results show very good performance in terms of sensitivity, flexibility of usage, and ultra-low weight, making PiezoPaint™ technology an attractive alternative for SHM particularly in aerospace applications.

1. INTRODUCTION

With the potential of replacing scheduled maintenance with as-needed maintenance, increasing vehicle lifetimes, discovering unpredicted damages, and increasing safety, the awareness on prognostics and health management has increased significantly in recent years (Raghavan & Cesnik 2007).

An essential part of prognostics and health management is structural health monitoring (SHM) which has been extensively studied in recent years (Raghavan & Cesnik 2007). The SHM field can be divided into two sub fields, passive and active SHM. Active SHM involves the use of actuators and sensors while passive SHM only applies sensors. Different sensing techniques are applied for SHM including fiber Bragg gratings, accelerometers and piezoelectric transducers (Liu & Nayak, 2012). In aerospace, the most useful SHM techniques are vibration-based approaches and guided wave based approaches (Liu & Nayak, 2012). The biggest challenges for SHM in aerospace in particular, are weight, wiring, and space availability.

Ultrasonic techniques are known to be very powerful and versatile for non-destructive testing of structural components and in the case of plate-like structures they generally rely on Lamb waves (Ringgaard, Zawada, Porchez, Bencheikh & Claeyssen, 2011). The full ultrasonic analysis needed to detect relevant defects is quite complex, since the various modes of the Lamb waves are dispersive and for example an extensive mode conversion may take place at interfaces between the various layers of a sandwich composite structure. In recent years the use of composite materials based on CFRP (carbon-fibre reinforced polymer) has increased dramatically in the aerospace industry. CFRP/honeycomb sandwich structures are characterised by a very high specific strength and stiffness compared to aluminium and other conventional structural materials. An additional advantage is that these materials are damage tolerant within certain limits (Hillger, Szewieczek, Schmidt, Sinapius, Aldave, Bosom, & Gonzalez, 2012). However, from the point of view of structural health monitoring, there are a number of issues complicating the matter. To begin with, such sandwich structures are sensitive to impacts of relatively low energy, and furthermore the resulting damage in the core is generally much more severe than the skin damage.

Typically, bulk piezoelectric materials are used for ultrasound-based NDT and SHM applications, however, such an approach has a number of limitations and drawbacks, such as high weight of the system, difficulties with integration of the sensor system into the structures, low compliance, and limited flexibility of application (Schäfer &

Janovsky, 2007). There has been an effort to use other classes of piezoelectric materials in order to address some of the above mentioned challenges, e.g. by using polyvinylidene fluoride (PVDF) family materials (Rao, Bhat, Murthy, Madhav, & Asokan, 2006). They are lightweight and can be applied to large areas. However, these polymer materials typically show low piezoelectric activity, are difficult to integrate with the structures, and pose several practical limitations in terms of wiring and processing, such as limited suitability for commercially available printing techniques. A noticeable degradation of dielectric- and piezoelectric properties of PVDF type films with the time, when the film is exposed to elevated temperatures (50-60 °C) has also been reported recently by Silva, Costa, Sencadas, Paleo, and Lanceros-Méndez (2011), which in turn limits the application of such films in aerospace industry.

In this work the functionality of a novel acoustic sensor array based on a flexible, printable piezoelectric material PiezoPaint™ is demonstrated. PiezoPaint™ technology alleviates or completely eliminates the drawbacks of bulk impact detection systems such as weight, complicated wiring and wave coupling, while offering higher piezoelectric response than PVDF. In addition it is compatible with commercially available printing techniques such as screen-printing and pad-printing. In essence the material is a 0-3 composite consisting of PZT particles and a polymer matrix.

In order to illustrate in practise the unique advantages of directly printed acoustic sensors the four-element sensor array based on PiezoPaint™ printed on an aluminium plate has been used for impact detection. A time difference of arrival (TDOA) algorithm has been applied for processing. Due to the direct integration of the sensors with the structure a very good sensitivity has been obtained, enabling accurate impact detection together with estimation of the impact energy. Kim, DeFrancisci, Chen, Rhymer, Funai, Delaney, Fung, Le, & White (2012) work with three sources of impacts on aircrafts. Impacts from ground service equipment which is usually high energy ($10^2 – 10^3$ J) high contact area impacts, high velocity ice e.g. hail impacts at in-flight speeds, and low velocity impacts from generic sources e.g. dropped equipment. In this study low velocity impacts were generated to test the demonstrators. Preliminary test results on a CFRP multilayer plate are presented as well.

2. PRINTABLE PIEZOELECTRICS

In recent years, a number of attempts have been made to combine piezoelectric bulk materials and polymers, developing ceramic-polymer composite materials (Payo & Hale, 2010), however, in most cases such materials represent bulk composite materials that are not suitable for printing techniques, require high curing temperatures, are rigid in a cured state, and therefore cannot be applied to a variety of substrates, including CFRPs.

In order to keep the advantages of both bulk and polymer piezoelectric materials a new flexible piezoelectric material, PiezoPaint™, has been developed by Meggitt A/S[1]. It has been developed primarily with the aim of keeping high piezoelectric activity while making it compatible with different substrates and structures, including textiles, plastics, metals, composites, paper, etc., and the ability to be applied to large areas by using commercially available printing techniques, including but not limited to pad-, screen-, or stencil printing. An important goal that has been targeted when developing PiezoPaint™ material was also to keep as low a processing temperature as possible, limiting it to 120 °C, making the PiezoPaint™ compatible with more materials including CFRP.

PiezoPaint™ represents a composite material that consists of an organic vehicle (polymer matrix) and a piezoelectric powder, manufactured on the basis of commercially available piezoceramic. Typically, hard PZT materials (e.g. Meggitt's Ferroperm™ Piezoceramics Pz24 or Pz26 piezoceramics) are used for manufacturing PiezoPaint™, with a different volume content of the piezoelectric powder in the polymer matrix, depending on the final application. However, lead-free piezoelectric materials have also been demonstrated, showing reasonable performance of PiezoPaint™ material, manufactured on the basis of these materials (see Table 1).

Normally, PiezoPaint™ is prepared in the form of a paste, which could be applied to a number of different structures by using pad-, screen-, and stencil printing techniques. The viscosity and overall fluidity of the paste can be adjusted, depending on the deposition technique.

Typical properties of different PiezoPaint™ materials, in comparison with PVDF based co-polymer material is shown in Table 1.

Table 1 shows that in comparison with PVDF type co-polymers, PiezoPaint™ materials exhibit higher piezoelectric activity (more sensitive in the case of sensor application), have a higher dielectric constant that can be tuned (by using different ratio between polymer matrix and piezoelectric powder, or by utilizing different type of piezoelectric powder with either high or low dielectric constant), and can be utilized at higher temperatures.

As it has already been mentioned above, the properties of PiezoPaint™ materials can be tuned, depending on the final application, e.g. the dielectric constant or compliance can be adjusted to simplify the impedance matching or feasibility of integration with different structures, where the sensor on the basis of PiezoPaint™ material is to be applied.

[1] Patent pending

The microstructure of PiezoPaint™ material screen-printed on alumina substrate and silver bottom electrode is shown in Figure 1. It is shown that PiezoPaint™ material in a cured state has a relatively dense structure, with very low porosity and very fine grain structure (comparing with other similar composite structures, see e.g. work by Arlt K., and Wegener M., (2010)).

An example of PiezoPaint™ materials deposited onto different substrates (polymer, PCB, fabric) by using commercial screen printing technique is shown in Figure 2. These structures are relatively simple. The PiezoPaint™ is sandwiched between the top and the bottom electrodes. The electrodes are based on a commercially available silver paste that can be applied by using the same printing techniques. However, when the material is deposited onto very rough substrates such as textile, an additional interface layer is necessary.

Table 1. Properties of PiezoPaint™ (PP) materials in comparison with piezoelectric polymer material (Omote et al, 1997)

Material	PVDF	PiezoPaint™ PP-50B	PiezoPaint™ PP-50LF
Type	Co-polymer	PZT Composite	Lead-Free Composite
ρ, g/cm3	1.8	5.2	< 4
T_{op}, °C	< 90	< 150	< 150
ε	10 – 12	125	250
tan δ, %	-	3.0	4.0
d_{33}, pC/N	-38	45	25

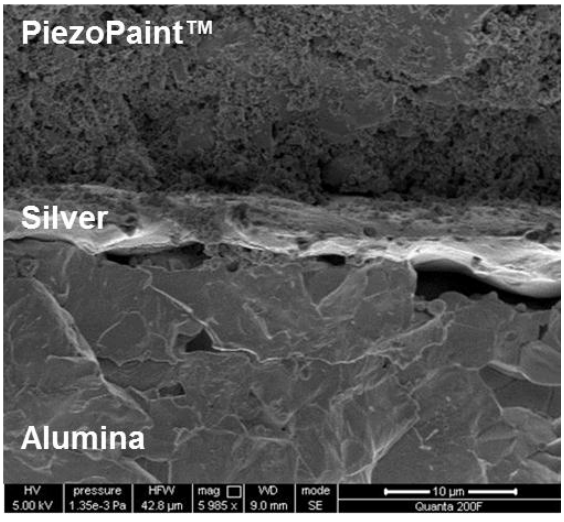

Figure 1. Microstructure (SEM image) of PiezoPaint™ material printed on alumina substrate.

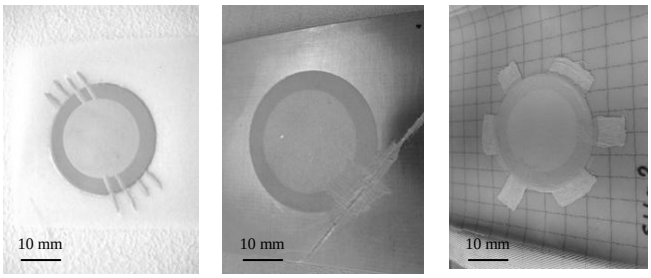

a) b) c)

Figure 2. Examples of PiezoPaint™ materials deposited on different substrates: a) – polymer, b) –PCB, and c) – fabric.

3. Sensor Arrays

The test structure consists of circular sensors forming a square array on an aluminium plate. The sensors have been placed at the corners of the plate. The sensor positions can be optimized for impact estimation as in (Staszewski, Worden, Wardle, & Tomlinson, 2000). However, a simpler configuration of the sensors has been chosen as a proof of concept approach. By principle only 3 sensors are needed for simple triangulation but for this demonstration 4 sensors were used. This allows 4 location estimations to be carried out for each impact instead of only 1, making the system more reliable.

3.1. Screen Printing

Screen printing is a well-known pattern transfer technique where a viscous medium is pressed through a woven mesh with a squeegee to generate a sharp edged pattern. The technique is widely used in many branches of industry, e.g. fabric printing industry, but it has also found its way into the electronics industry (hybrid electronics). In this study screen printing was used to print the PiezoPaint™ and the top electrodes, forming the structure of the sensor. The basic process is shown in Figure 3.

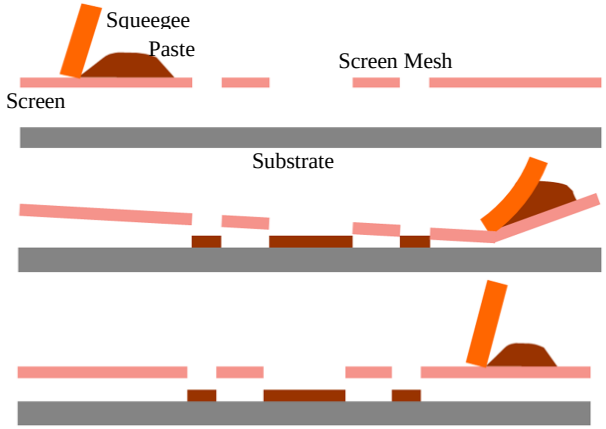

Figure 3. Basic screen printing process.

3.2. Fabrication of demonstrator on aluminium plate

The impact detection demonstrator has been fabricated by printing PiezoPaint™ based sensors at the corners of an aluminium plate (20 cm x 30 cm x 0.5 cm), 2.5 cm from either side.

The sensors have been made as sandwiched structures with the aluminium plate serving as bottom electrode, and a commercial silver paste (Dupont Ag 5028) printed on top of an active layer serving as the top electrode. The diameters of the sensor patches were 12 mm while the top electrode diameters were 10 mm making the active transducer diameter 10 mm. A cross section of the deposited transducers is shown in Figure 4.

The following procedure has been used to fabricate the demonstrator.

- The PiezoPaint™ has been deposited using a commercial screen printer.
- Dupont Ag 5028 has been deposited on top of the PiezoPaint™ patches also using the screen printer.
- Poling has been carried out using a high electrical field (above 1.5. kV/mm) between the top and bottom electrode at an elevated temperature (above 60 °C).
- Wiring has been made at each location using an intermediate printed circuit board (PCB), and conductive epoxy.

The demonstrator with the PCB connectors is shown in Figure 5.

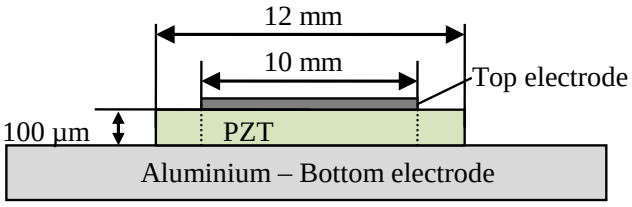

Figure 4. Cross section view of the PiezoPaint™ sensor.

a) b)

Figure 5. a) The aluminium impact detection demonstrator. b) The PCB used to connect the sensor to a coaxial cable.

4. EXPERIMENTAL PROCEDURE

To evaluate the functionality of the PiezoPaint™ based sensors impact detection experiments have been performed. The experiments have been conducted by connecting the sensor output signal directly to a four-channel oscilloscope (Agilent Infiniium Oscilloscope DSO8064A). Time difference of arrival (TDOA) method has been used to estimate the impact locations.

4.1. Test setup

Impact detection tests were carried out using the setup shown in Figure 6 and Figure 7. Each sensor was connected to a port of the oscilloscope and the oscilloscope was set to take a single waveform acquisition with the trigger set up on channel 1. The impact detection location was estimated after data collection; however, a continuous impact monitoring is possible in real application. In order to control the location and the magnitude of the impacts the following setup was used. A tube with an array of small holes with 1 cm spacing was secured 1 cm above the plate. A pin was used to hold a steel ball in place inside the tube. When the pin was released the ball dropped at a chosen location from a certain height. This setup is shown in Figure 7. The impact energy is estimated by calculating the potential energy of the ball at a certain height and assuming that half of the energy is transferred into the plate at impact, causing deformation and propagating waves.

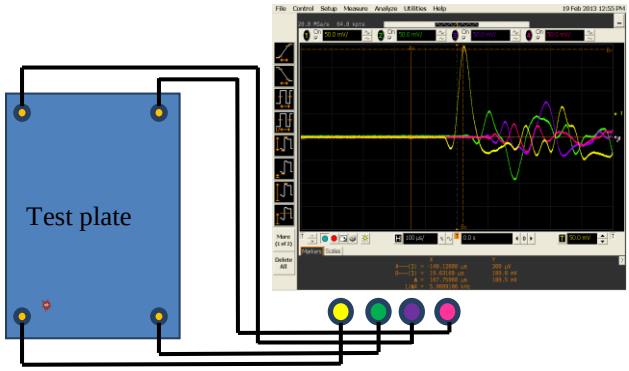

Figure 6. Measurement setup for impact detection experiments.

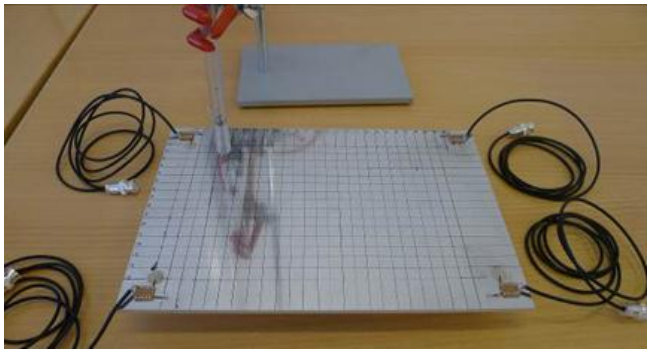

Figure 7. Setup for generating controlled impacts in known locations.

4.2. Time Difference of Arrival

Time difference of arrival (TDOA) is widely used in source localization and finds applications in GPS and cellular location (Patwari, Ash, Kyperountas, Hero III, Moses, & Correal, 2005). It employs three or more receivers to accurately compute the position of an emitter. In this study TDOA is used to estimate the location of an impact. An impact on any surface generates ultrasonic waves that propagate through the medium. The time difference of arrival of these waves at the sensor locations can be used to estimate the impact location. Knowing the speed of sound in the substrate the time differences can be used to calculate distance differences Eq. (1).

$$\Delta t_{21} \cdot v = |\Delta r_{21}| \qquad (1)$$

Where Δt_{21} is the time difference of arrival between sensor 1 and 2, v is the speed of sound in the substrate and Δr_{21} is the difference in distance between the two sensors and the impact.

Eq. (2) shows how the locations of sensor 1, sensor 2 and the impact relate to the distance difference.

$$|\Delta r_{21}| = |r_2| - |r_1| \Leftrightarrow$$
$$|\Delta r_{21}| = \sqrt{(x_2 - x_{im})^2 + (y_2 - y_{im})^2} - \sqrt{(x_1 - x_{im})^2 + (y_1 - y_{im})^2} \qquad (2)$$

Where $|r_1|$ and $|r_2|$ are the distances between the impact and sensors 1 and 2 respectively, and x_1, y_1, x_2, y_2, x_{im}, y_{im} are the x-y components of the sensors and the impact location respectively. Depending on the number of applied sensors a set of equations like Eq. (2) can be created. These equations represent non-linear hyperbolas; however the impact locations can be estimated by applying numerical methods such as the least-squares method (Yang, An, Xu (2008)).

Figure 8 shows the distance between the impact and the sensor and the hyperbolas represented by Eq. (2).

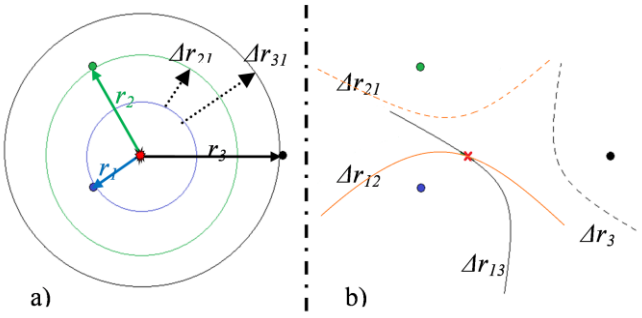

Figure 8. a) 3 receivers and emitter where r_1, r_2 and r_3 are the distances between the emission and the receivers. b) Hyperbolas intersect at the emission location marked by the red x.

4.3. Data Analysis

The TDOA algorithm has been implemented using *Octave*. The program first estimated the arrival times of the propagating waves generated by the impact, at the four sensor locations. To determine when a wave arrived at a sensor a threshold voltage was chosen. The threshold was set to 25 % of the maximum amplitude. This threshold value was chosen based on the best results from impact localization tests. This choice sets a lower limit on the signal to noise ratio required to achieve a useable signal.

$$SNR = \left(\frac{A_{signal}}{A_{noise}}\right)^2 = (4)^2 = 16 \text{ or}$$
$$SNR_{\text{dB}} = 20\log_{10}(4) = 12.04 \text{ dB}$$

The amplitude of the noise was around 15 mV during the measurements which, with a 25 % threshold implied a minimum detectable voltage amplitude at the level of 60 mV. For comparison a 4 g steel ball dropping at the corner furthest away from sensor 1 lead to a maximum voltage amplitude of 100 mV as shown in Figure 9. This corresponds to a signal to noise ratio of 16.48 dB.

After estimating the time of arrival, the script applied the estimated time differences to solve the nonlinear equations numerically and plot the estimated locations with the actual locations.

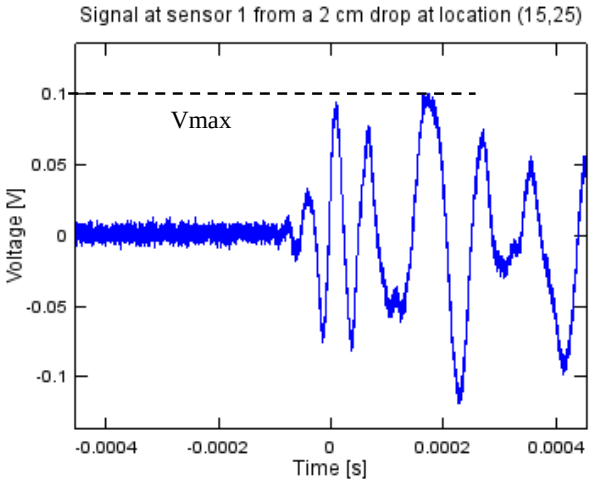

Figure 9. The voltage output at sensor one for a 2 cm drop. The maximum amplitude is 100 mV.

4.4. Experimental Results

4.4.1. Impact Energy

In order to assess the sensitivity of the printed sensors as well as the correlation of the output signal with the impact energy a steel ball with a mass of 4 g was dropped from fixed heights as close to sensor one as possible without landing on top of it. A voltage amplitude reading is shown

in Figure 10 and the results from various drop heights are plotted in Figure 11.

Figure 11 shows that a linear fit can be made between the transferred momentum and the voltage amplitude for this specific case with R^2=0.97. The drop height can also be used to estimate the impact energy.

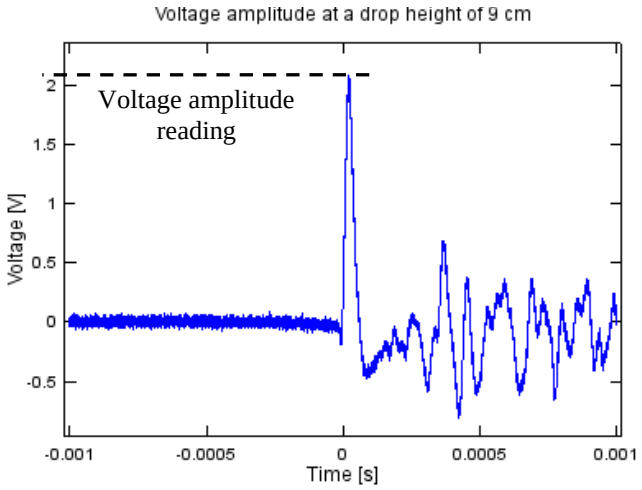

Figure 10. The measured voltage signal (9 cm drop).

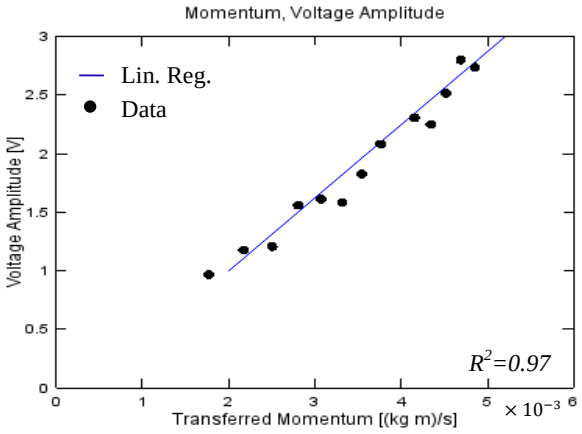

Figure 11. Output voltage amplitude as a function of transferred momentum.

4.4.2. Impact Localisation

In total, 153 impacts were captured across the plate. Results from the initial tests are shown in Figure 13. In Table 2 the average estimation error as a measure of accuracy is shown. More than 90 % of the impacts were located with an error smaller than 5 cm. For comparison Schäfer & Janovsky (2007) work with an impact location accuracy requirement of ~5 cm for hypervelocity impacts on spacecraft. Only 1 impact was discarded as it was completely off the plate.

Table 3 shows the error depending on impact positions and drop height. From Table 3 it is noted that the accuracy tends to depend on the position of the impact. Along the bottom edge of the plate (b in Figure 12) the location estimation is less accurate. Drop height does not seem to affect the accuracy in this specific case. However, the sample size is small and all impact velocities can be considered low (Kim, H. et al., (2012)).

The results bode well for future application, and with optimization of the impact estimation algorithms it is believed that the errors can be reduced significantly.

Table 2. Accuracy of impact location estimations.

	Error <5 cm	Error <7.5 cm	Error <10 cm	Error <12.5 cm	All
#	138	149	151	153	153
%	90.2	97.4	98.9	99.3	100

Table 3. Accuracy of impact location estimations depending on drop height and impact positions. Impact positions are illustrated in Figure 12. “Forced” means the plate was hit by hand with the steel ball.

Positions	Drop Height [cm]	Error < 5 cm [%]	Error < 7 cm [%]
Along line a	3	96 (23/24)	100 (24/24)
Along line b	3	93 (13/14)	93 (13/14)
Along line c	3	86 (12/14)	100 (14/14)
Along line a	7	92 (22/24)	100 (24/24)
Along line b	7	86 (12/14)	86 (12/14)
Along line c	7	86 (12/14)	100 (14/14)
Along line a	15	96 (23/24)	100 (24/24)
Random	15	88 (15/17)	94 (16/17)
Random	Forced	75 (6/8)	100 (8/8)

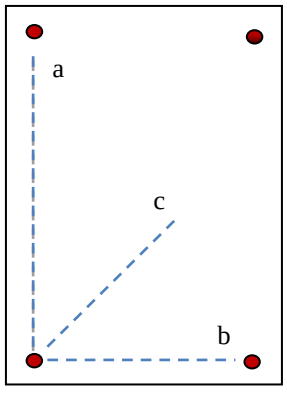

Figure 12. Impact positions used in the drop tests.

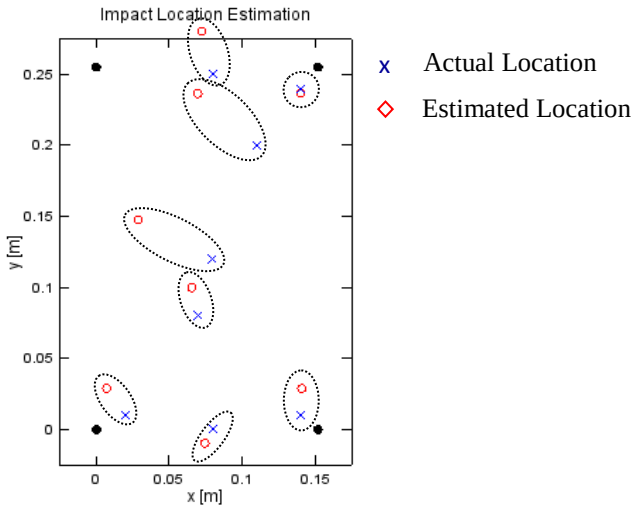

Figure 13. Results from impact localisation of random forced impacts. The dotted cylinders indicate which actual – and estimated location pairs belong together.

4.4.3. CFRP - Preliminary Results

In addition to the aluminium demonstrator a CFRP impact detection demonstrator has been fabricated. The composite plate (40 cm x 40 cm x 1.35 cm) consists of an anti-symmetric honeycomb sandwich structure with a skin thickness of 1 mm and 0.5 mm respectively, and an integrated bronze mesh for lightning protection.

The sensor size and placements are shown in Figure 14. The sensors are placed in the corners of the CFRP plate 4 cm from each side. Instead of connecting at each sensor node electrical connections were painted with Dupont Ag 5028, and wiring was done at a single location as shown in Figure 14. The setup for preliminary impact location tests is shown in Figure 14. Tests have been carried out similarly to the tests of the aluminium demonstrator.

The preliminary results based on 14 impacts with the light hammer are listed in Table 4 and an example of an impact localisation is shown in Figure 15.

Near-future work with this includes energy estimation and the effect on localisation accuracy, effect of impact surface, and effect of impact position on accuracy.

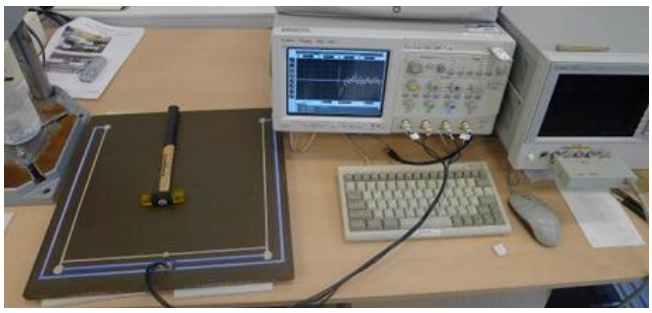

Figure 14. Setup for impact testing on the CFRP plate.

Table 4. Accuracy of impact localisation on CFRP based on the preliminary tests.

	Error < 2.5 cm	Error < 5 cm	All
#	5	14	14
%	35.7	100	100

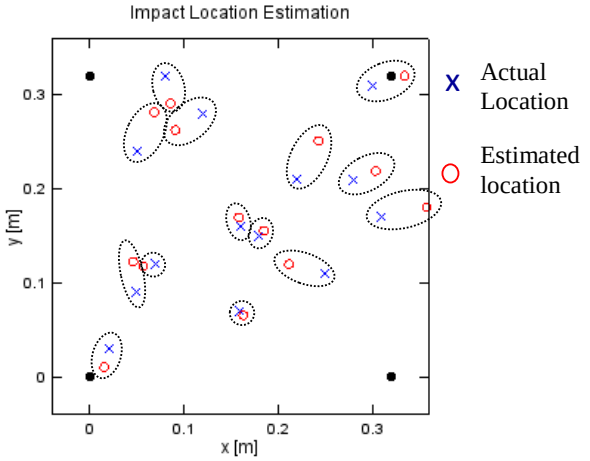

Figure 15. Location estimation on the CFRP plate. The dotted cylinders indicate which actual –and estimated location pairs belong together.

5. Discussion

For an impact detection system to be a viable SHM solution energy estimation is critical. It will enable the system to supply the users with information on the damage extent after impacts, and whether maintenance is needed.

In this study it was shown that the energy can be estimated when the impacts are from a 4 g steel ball at low velocities. However, different geometries and material properties of the impacting objects will influence the generated waves, and thereby the estimated energy.

Thorough studies of impacts from plausible objects and materials e.g. hail, are needed, and should be held up to studies of the damages generated in composites from impacts.

6. Conclusions

- A sensor array based on PiezoPaint™ technology has been successfully developed and demonstrated.
- The sensor system has been directly deposited on aluminium as well as CFRP honeycomb structure, overcoming the typical problems of sensor integration.
- Due to the high sensitivity of the piezoelectric material as well a as the direct contact between the sensing material and the structure the measured output voltage

signal is relatively strong (in the range of volts) and can be directly used for impact detection and localisation without additional signal conditioning.

- According to the experimental data the average detection error was not exceeding 5 cm in the case of an aluminium plate of 20 cm x 30 cm x 0.5 cm and a 4 g steel ball.
- The near–linear dependence of the maximal signal amplitude on the transferred momentum suggests that the printed sensor array can be successfully applied in impact energy estimation, as well.
- Printing of the whole wiring system is a natural extension of the presented technology. The preliminary tests of CFRP sensor array with printed conductors show very good performance.
- It has been shown that the weight and the complexity of SHM system based on acoustical sensors can be significantly reduced by using printed piezoelectric material (PiezoPaint™), while keeping the high sensitivity of the sensors.

ACKNOWLEDGEMENT

Karl Elkjaer would like to acknowledge the Meggitt Graduate Programme for supporting the work.

The authors would also like to thank colleagues at Meggitt A/S for their help and valuable feedback.

REFERENCES

Arlt, K., & Wegener, M., (2010), Piezoelectric PZT/PVDF-copolymer 0-3 composites: Aspects on film preparation and electrical poling, *Dielectrics and Electrical Insulation, IEE Transactions*, 17 (4), 1178-1184, Doi: 10.1109/TDEI.2010.5539688

Baskar Rao, M., Bhat, M.R., Murthy, C.R.L., Venu Madhav, K., & Asokan, S., (2006). Structural health monitoring (SHM) using strain gauges, PVDF film and fiber bragg grating (FBG) sensors: A comparative study, Proc. National Seminar on Non-Destructive Evaluation, Dec.7-9, Hyderabad.

Hillger, W., Szewieczek, A., Schmidt, D., Sinapius, M., Jorge Aldave, I., Venegas Bosom, P. & Vega Gonzalez, L. (2012). Advanced NDT techniques for damage detection in a honeycomb composite helicopter tailboom, Proc. on 5th International Conference on Emerging Technologies of Non-Destructive Testing (ETNDT5), Ioannina, Greece, 19th – 21st September 2011

Kim, H., DeFrancisci, G., Chen, Z. M., Rhymer, J., Funai, S., Delaney, M., Fung, S., Le, J., & White, S., (2012) Impact damage formation on composite aircraft structures, UCSD FAA JAMS Paper, Project Description Paper Supporting Presentation Given at Federal Aviation Administration JAMS 2012 Technical Review Meeting 5 April 2012, Baltimore, MD

Liu, Y., & Nayak, S., (2012). Structural health monitoring: State of the art and perspectives, *JOM* 64 (7), 789-792, Doi: 10.1007/s11837-012-0370-9

Omote, K., Ohigashi, H., & Koga, K., (1997). Temperature dependence of elastic, dielectric, and piezoelectric properties of "single crystalline" films of vinylidene fluoride trifluoroethylene copolymer, *J. Appl. Phys.*, 81, 2760-2769. Doi: 10.1063/1.364300

Patwari, N., Ash, J. N., Kyperountas S., Hero III, A. O., Moses, R. L., & Correal, N. S., (2005). Locating the nodes: Cooperative localization in wireless sensor networks, *IEEE Signal Processing Magazine*, 22 (4), 54-69. Doi: 10.1109/MSP.2005.1458287

Payo, I. & Hale, J.M., Dynamic characterization of piezoelectric paint sensors under biaxial strain, (2010). *Sensors and Actuators A*, 163, 150-158, Doi: 10.1016/j.sna.2010.08.005

Raghavan, A., & Cesnik, E. S., (2007). Review of guided-wave structural health monitoring, *The Shock and Vibration Digest*, 39 (2), 91-114. Doi: 10.1177/0583102406075428

Ringgaard, E., Zawada, T., Porchez, T., Bencheikh, N., & Claeyssen, F., (2011) Multi-element piezo-composite transducers for structural health monitoring using Lamb waves, Proc. on 5th International Conference on Emerging Technologies of Non-Destructive Testing (ETNDT5), Ioannina, Greece, 19th – 21st September 2011

Schäfer, F., & Janovsky, R., (2007). Impact sensor network for detection of hypervelocity impacts on spacecraft, *Acta Astronautica*, 61, 901-911, Doi: 10.1016/j.actaastro.2007.02.002

Silva, M. P., Costa, C. M., Sencadas, V., Paleo, A. J., & Lanceros-Méndez, S., (2011). Degradation of the dielectric and piezoelectric response of β-poly(vinylidene fluoride) after temperature annealing, *Journal of Polymer Research*, 18 (6), 1451-1457. Doi: 10.1007/s10965-010-9550-x

Staszewski, W. J., Worden, K., Wardle, R., & Tomlinson, G. R. (2000). Fail-safe sensor distributions for impact detection in composite materials. *Smart Materials and Structures*, 9 (3), 298-303. Doi:10.1088/0964-1726/9/3/308

Yang, K., An, J., & Xu, Z. (2008), A quadratic constraint total least-squares algorithm for hyperbolic location, *I.J. Communications, Network and System Sciences*, 2, 130-135. Doi: 10.4236/ijcns.2008.12017

Karl Elkjaer received his BSc (2009) and MSc (2011) in Physics and Nanotechnology from the Technical University of Denmark. His master thesis involved designing, fabricating and testing a biochip for investigation of transport

through cells and cell membranes. In 2011 he joined the R&D department at Meggitt Sensing Systems Denmark, where he worked on a customer sponsored project concerning high intensity focused ultrasound for treatment of glaucoma. He is currently working on a project concerning structural health monitoring applications of a newly developed material - PiezoPaint™.

Konstantin Astafiev is an R&D Project Manager at Meggitt A/S with the main field of activity in the area of environmentally friendly piezoelectric materials, flexible piezoelectric materials and composites, and piezoelectric thick films. He authored and co-authored over 40 scientific papers and conference articles and holds MSc in Electronics and Microelectronics (2000) and PhD in Materials Science (2004). He has extensive experience in international work, being involved in a number of EC and nationally funded projects.

Erling Ringgaard is Principal Materials Scientist at Meggitt A/S and has more than 15 years of experience in the field of piezoelectric ceramics (M.Sc. in chemistry, PhD in materials science). He authored and co-authored over 60 scientific papers and conference articles. He has participated in a number of EC-funded RTD projects and been the coordinator of two of these. Currently he is the project leader of a nationally funded project on energy harvesting.

Tomasz Zawada, holds MSc degree in Electronic Engineering (2000), PhD degree in Microelectronic Engineering (2004) and MBA degree in Management of Technology (2012). He has more than 10 years of experience in academic and industrial research in the fields of ceramic microsystems, microfluidics, piezoelectric materials and devices. He has authored and co-authored more than 60 scientific publications and reports. Currently, he is working as Engineering and Research Manager at Meggitt A/S, Denmark. His main professional interest is focused on applications of piezoelectric thick films in sensors, transducers and energy harvesting.